Magneto-optical and magnetization studies in the rare-earth orthochromites. VI. $NdCrO_3$

R. M. Hornreich, Y. Komet,* and R. Nolan†
Department of Electronics, The Weizmann Istitute of Science, Rehovot, Israel

B. M. Wanklyn
Clarendon Laboratory, Oxford, England

I. Yaeger‡
Department of Electronics, The Weizmann Institute of Science, Rehovot, Israel
(Received 24 February 1975)

Single crystals of $NdCrO_3$ were studied by means of bulk magnetization, susceptibility, and optical-absorption spectroscopy measurements. This compound orders at $T_N = 214$°K in a $\Gamma_2(F_x)$ canted antiferromagnetic spin structure which persisits down to $T_R = 35$°K. At T_R a first-order Morin-type phase transition occurs and, down to below 4.2°K, the spins are in the antiferromagnetic $\Gamma_1(0)$ mode. The temperature dependence of the spontaneous magnetization above T_R is significantly different from that of other rare-earth orthochromites and is reminiscent of that found in some ferrimagnetic materials. Using a single-ion model in the molecular-field approximation, it is shown that this behavior is due to magnetization contributions from the two lowest Kramers's doublets of the Nd^{3+} ground multiplet. The calculated Stark splitting is 97 ± 15°K, in excellent agreement with the absorption spectroscopy measurements. Above T_R, the ground-doublet splitting is essentially due to the Nd-Cr interaction, while below T_R the additional polarization due to Nd-Nd coupling becomes significant.

I. INTRODUCTION

The compound $NdCrO_3$, in conformity with other rare-earth orthochromites, crystallizes in an orthorhombically distorted perovskite structure (space group *Pbnm*) with four formula units per unit cell.[1] The exchange coupling between the magnetic moments of the Cr^{3+} nearest neighbors is predominantly antiferromagnetic and they order magnetically at a Néel temperature of $T_N = 214$°K. Below this temperature and down to approximately 35°K, $NdCrO_3$ exhibits a weak ferromagnetic moment.

The magnetic properties of $NdCrO_3$ have been investigated previously using neutron diffraction,[2-4] specific-heat,[5,6] and bulk magnetization measurements,[6] all on powder samples. The results of the neutron-diffraction studies may be briefly summarized as follows: At 77°K the spin structure of the Cr^{3+} ions is, in the notation of Koehler *et al.* and Bertaut[7] primarily G_x; at 4.2 and 1.5°K the Cr^{3+} spins are in a mixed G_{xy} mode and the Nd^{3+} moments have a c_z structure.[8] The latter ordering appears below 13°K. The $NdCrO_3$ specific-heat measurements, carried out in the 4.2–15°K temperature region, show a Schottky anomaly typical of a two-level system with a splitting of 27°K. No evidence for a cooperative ordering of the Nd^{3+} spin system was found, indicating that this ordering is induced by a Nd-Cr rather than Nd-Nd interaction. Finally, the temperature dependence of the powder magnetization is strikingly different from that reported for other orthochromites with paramagnetic rare-earth ions.[9-13] Below $T_N = 224$°K, the magnetization increases with decreasing temperature, reaching a maximum value of 0.05 μ_B/spin at $T = 200$°K. It then decreases monotonously to a minimum value of 0.01 μ_B/spin at $T = 80$°K. As the temperature is further lowered, the magnetization again increases, reaching a maximum of 0.3 μ_B/spin at 35°K. Below this point the magnetization falls toward zero, although a small moment is still found at 4.2°K. Ayasse[6] has interpreted this behavior as indicative of a compensation point in the vicinity of 80°K and a spin-orientation phase transition from a high-temperature G_x spin mode to a low-temperature G_y mode at 35°K. The nature of the latter (i.e., first or second order) was not determined.

More recently, Belov *et al.*[14] have measured the spontaneous magnetization of $NdCrO_3$ single crystals. They report a Néel temperature of 240°K, below which the weak ferromagnetic moment is along the *a*-crystallographic axis. This implies that the ordered Cr^{3+} spins are in a G_zF_x mode and is not in agreement with the neutron-diffraction results. They further find that the ferromagnetic moment reverses sign at 87°K, as it should at a true compensation point.[9] At still lower temperatures, the magnitude of the spontaneous magnetization again increases, reaches a peak at approximately 35°K, and decreases to zero at 10°K. Below 10°K no net moment was found, and this is consistent with G_y and c_z structures for the Cr and Nd spin systems, respectively.

From the above summary of the results of previous studies on $NdCrO_3$ it is clear that the experimental data are not completely consistent with

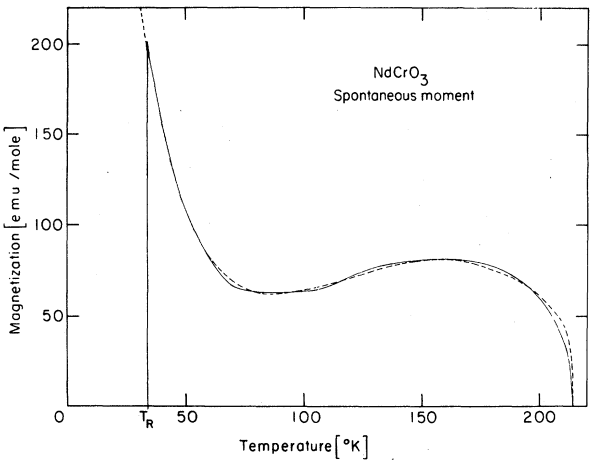

FIG. 1. Temperature dependence of the spontaneous magnetization of $NdCrO_3$. The experimental data are corrected for demagnetizing effects. (The experimental results are given by the solid line and the theoretical fit by the dashed line.) The measured moment is along the a crystallographic axis between $T_R = 34\,^\circ$K and $T_N = 214\,^\circ$K and vanishes between 4.2 °K and T_R.

each other. Furthermore, there has been neither a completely satisfactory explanation for the reported magnetic behavior nor any quantitative analysis of the experimental results. In this paper, we shall therefore give a detailed analysis of the magnetic behavior of $NdCrO_3$. This analysis will be based on our extensive magnetic and magneto-optical studies of this compound.

In Sec. II, we first outline the various measurements performed and present the experimental results of the optical absorption and bulk magnetization and susceptibility studies. A part of the optical data has been reported previously.[15] Next, in Sec. III, we analyze the experimental data for each of the phases studied and for the observed phase transition. Finally, in Sec. IV, the results of the data analysis are summarized and our conclusions regarding the nature of the Cr-Nd and Nd-Nd interactions are presented.

II. EXPERIMENTAL RESULTS

Our studies were carried out on flux-grown single crystals of $NdCrO_3$. The crystallographic axes were identified by a knowledge of the symmetry and morphological features of the crystals.[1,16] Details of the systems employed for the magnetic and optical measurements have been given elsewhere.[12]

A. Magnetic measurements

The measured spontaneous magnetization of $NdCrO_3$ is shown in Fig. 1. Between an ordering temperature of $T_N = 214 \pm 1\,^\circ$K and down to $T_R = 34 \pm 1\,^\circ$K, the ferromagnetic moment was found to lie along the crystallographic a axis. The temperature dependence of the magnetization in this region is qualitatively similar to that reported by Ayasse.[6] However, the minimum in the magnetization found at $T \simeq 80\,^\circ$K cannot be regarded as evidence of a compensation point as the measured value (approximately 50 emu/mole) is well above the sensitivity threshold of the measuring system. At T_R, the magnetization along the a axis drops abruptly to zero and remains at this value down to 4.2 °K, the lowest temperature reached in our study. No net moment was found along any of the other crystallographic directions for $4.2\,^\circ\text{K} < T < T_R$. Thus unlike Ayasse[6] and Belov *et al.*[14] we find no spontaneous magnetization below T_R. This result was confirmed by measurements on several different crystals.

The magnetic susceptibilities measured along each of the principal crystallographic axes of $NdCrO_3$ from 4.2 to 215 °K are given in Fig. 2. No significant anomaly was found in any of the susceptibilities in the vicinity of T_N. At T_R, however, each of the three susceptibilities exhibited a step-like discontinuity. This discontinuity was particularly large in the case of the a-axis susceptibility.

B. Spectroscopic measurements

For the optical part of our study, a (110) platelet of $NdCrO_3$ polished down to a thickness of 50 μm was prepared. Relative absorption spectra were recorded as a function of wavelength for electric field polarizations, parallel and perpendicular to the crystal's c axis. The known complexity of the Nd^{3+} absorption spectrum in the visible and near infrared regions,[17] superimposed on the Cr^{3+} absorption spectrum, limited our work to a very narrow spectral region. We therefore concentrated on the Nd^{3+} absorption lines corresponding to transitions between the two lowest-lying crystal-field states of the $^4I_{9/2}$ ground term and excited-crystal-field states identified[17] as belonging to $^4G_{7/2}$. Since each crystal-field Kramers doublet is further split by the magnetic interactions, the absorption spectra consisted of subgroups, each containing a maximum of four absorption lines.

The spectroscopic measurements were carried out between 15 and 160 °K. At $35.1 \pm 0.5\,^\circ$K, a sharp change in the character of the spectra was noted. This may be seen in Fig. 3, where we present absorption spectra recorded at 34 and 36 °K. Figure 3 shows transitions between the lowest lying Kramers doublet of $^4I_{9/2}$ and all four of the Kramers doublets belonging to $^4G_{7/2}$. The actual width of the transition region was no more than 0.1 °K and the transition is, accordingly, very probably of first order. Note that the transition temperature is in excellent agreement with the $34 \pm 1\,^\circ$K value observed in the magnetic studies.

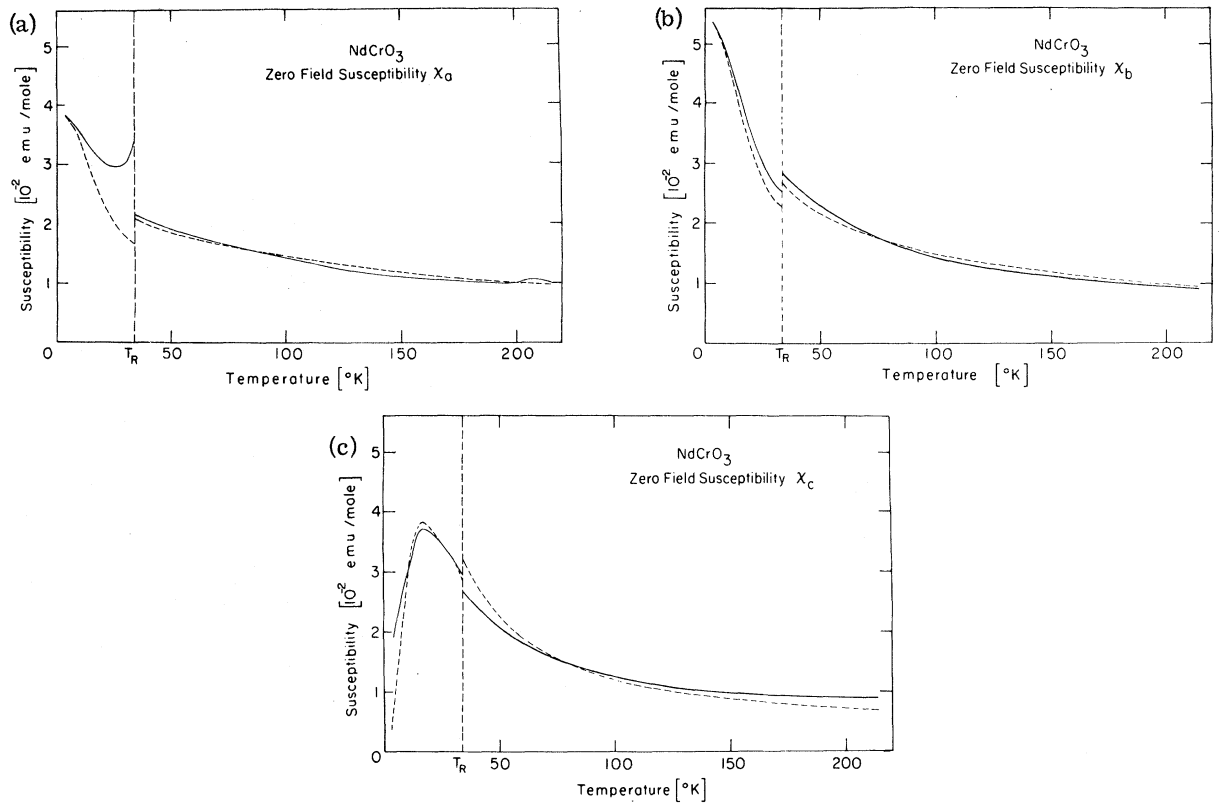

FIG. 2. Temperature dependence of the principal susceptibilities of $NdCrO_3$ along the (a) a, (b) b, and (c) c crystallographic axes. The experimental data are corrected for demagnetizing effects. (The experimental results are given by the solid line and the theoretical fits by the dashed lines.)

The notation in Figs. 3 and 4, is that of Faulhaber *et al.*[18] wherein the crystal-field levels of the ground term are labeled with roman numerals (I, II, ...) and those of the excited terms with lower-case letters (a, b, ...) starting with "a" for the level with lowest energy. The spectral lines of Fig. 3 were recorded in the 5250- to 5320-Å wavelength region. Additional lines with much lower intensities were observed at 77 °K in the 5320- to 5350-Å region and are shown in Fig. 4. These additional lines were identified as transitions between doublet II of $^4I_{9/2}$ and doublets a and b of $^4G_{7/2}$. Note that the transitions IIc and IId are not identifiable in Fig. 4 since they fall in the same wavelength region as the much stronger Ia and Ib lines.

The experimental data for the temperature dependence of the ground doublet splitting, based on the $^4I_{9/2}(\mathrm{I}) \rightarrow {}^4G_{7/2}$ (a, b, c, d) transitions, are summarized in Fig. 5. At $T = T_R$ there is a distinct discontinuity in the splitting, in agreement with the change in the spectrum character shown in Fig. 3.

Finally, we note that external magnetic fields of up to 20 kOe, applied either parallel or perpendicular to the c crystallographic axis, had no visible influence on the observed spectra.

III. ANALYSIS

The results of the spectroscopic measurements presented in Sec. II complement those of the bulk magnetization studies. We consider first the question of the Cr spin structure.

The spontaneous magnetization for $T_N > T > T_R$ is along the a axis, indicating that the appropriate Cr spin structure assignment is $G_z F_x$, belonging to the Γ_2 representation of $Pbnm$.[7] Below T_R no spontaneous magnetization is found, a result consistent with the Cr spins being ordered in the antiferromagnetic G_y mode, belonging to Γ_1. Turning to the optical data, if the observed change in the spectra of Fig. 3 is indeed due to a Morin-type Cr spin reorientation from $G_z F_x$ to G_y as the temperature is lowered, we expect the effective field at the Nd ion sites due to the ordered Cr spin system to be along the c axis for $T < T_R$.[7] For such a situation, the selection rules between the exact crystal-field states are preserved below T_R and are lifted only above this temperature.[12,19] An inspection of the spectra of Fig. 3 shows that the

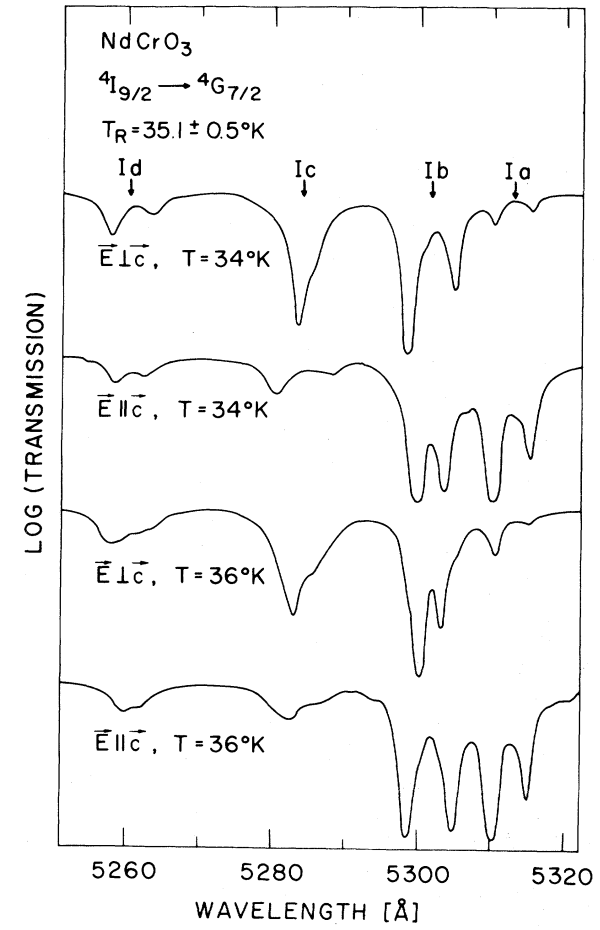

FIG. 3. Optical absorption spectra of Nd^{3+} in $NdCrO_3$ immediately above and below the spin reorientation temperature T_R for polarizations parallel and perpendicular to the c crystallographic axis. I refers to the lowest-lying Kramers doublet of the $^4I_{9/2}$ ground state, and a, b, c, d to the Kramers doublets of the $^4G_{7/2}$ excited state.

selection rules are indeed not strictly valid, for $T > T_R$. This is seen most distinctly in the Ib, Ic, and Id groups of transitions, where traces of the strong pair of absorption peaks in the $\vec{E} \perp \vec{c}$ spectrum are found also in the $\vec{E} \parallel \vec{c}$ spectrum and vice versa. These results are consistent with a $G_z F_x$ Cr spin mode. On the other hand, for $T < T_R$, an inspection of the same transitions shows that the selection rules are preserved. Each polarization shows a distinct pair of absorption peaks without any noticeable mixing taking place, in agreement with a G_y mode for the Cr spins.

The magnetic behavior of $NdCrO_3$ from ambient down to 4.2 °K can thus be summarized as follows: The Cr^{3+} moments order magnetically at a Néel temperature of $T_N = 214 \pm 1$ °K. Between T_N and $T_R = 35.1 \pm 0.5$ °K, the net magnetic moment is along the crystallographic a axis, indicating that the compound is in the Γ_2 phase with a $G_z F_x(Cr^{3+}) - c_y f_x(Nd^{3+})$ spin structure. More specifically, the Cr^{3+} moments are ordered predominantly antiferromagnetically parallel to the c axis with a small canting which results in a net moment along a. The Nd^{3+} moments are polarized by Cr-Nd exchange and dipolar interactions such that each of the moments lies in the ab crystallographic plane. These moments exhibit an antiferromagnetic alignment along the b axis and a ferromagnetic alignment along the a axis of the crystal. At T_R, an apparently first-order phase transition occurs to a low-temperature Γ_1 phase with the spin structure becoming $G_y(Cr^{3+}) - c_z(Nd^{3+})$.

We next turn to a quantitative analysis of the data presented in Sec. II. As pointed out earlier, the $NdCrO_3$ magnetization curve differs significantly from those typically found in the rare-earth orthochromites[9-13] and orthoferrites.[20,21] It is, in some respects, reminiscent of those found in

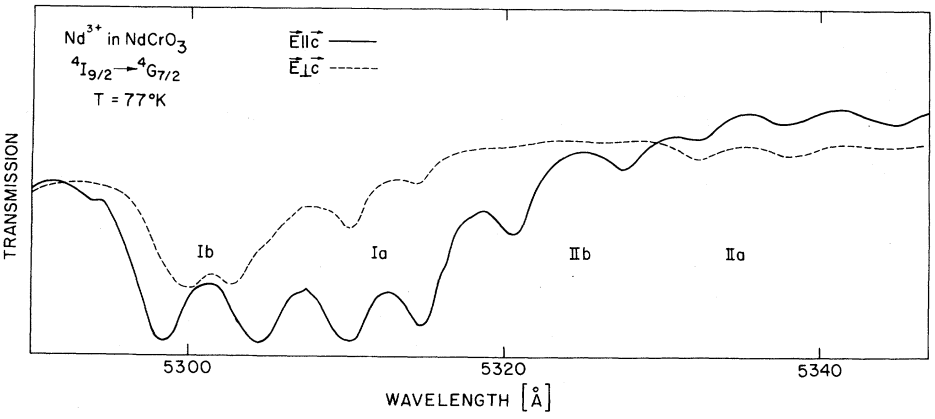

FIG. 4. Optical absorption spectra of Nd^{3+} in $NdCrO_3$ at 77 °K for polarizations parallel and perpendicular to the c crystallographic axis. I and II refer to the lowest-lying Kramers doublets of the $^4I_{9/2}$ ground state and a and b to the Kramers doublets of the $^4G_{7/2}$ excited state. The sets of four absorption peaks belonging, respectively, to Ia, Ib, and IIa are visible in the spectra. For IIb, only the two peaks in the $\vec{E} \parallel \vec{c}$ spectrum can be distinguished. The transition near 5345 Å was not identified.

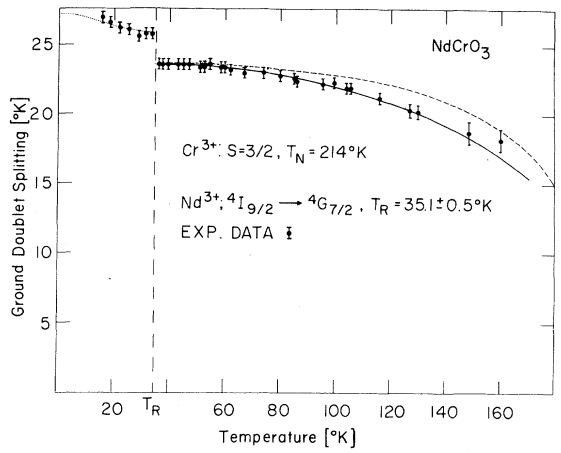

FIG. 5. Temperature dependence of the ground-doublet splitting of Nd^{3+} in $NdCrO_3$ in the $\Gamma_2(F_x)$ $(T > T_R)$ and $\Gamma_1(0)$ $(T < T_R)$ phases. The experimental points and estimated error are shown. The theoretical fits shown for $T > T_R$ are from a molecular-field calculation of $\langle S\rangle/S$ (solid line) and $\langle S\rangle/S$ as taken from the measured magnetization of $LuCrO_3$ (dashed line—see text). For $T < T_R$, the theoretical best fit is shown by the dotted line.

some ferrimagnets [e.g., $NiO \cdot Fe_{1.4}Al_{0.6}O_3$ (Ref. 22], rather than weak ferromagnets of the Dzialoskinsky type. To understand this behavior, it is useful to consider first the results of the optical-absorption measurements. From Fig. 5, we see that above T_R, the temperature dependence of the splitting of the ground Kramers doublet is well described by

$$\Delta E_g(T) = \Delta E_{g2}(0)(\langle S\rangle/S), \quad T > T_R\ , \tag{1}$$

where $\langle S\rangle/S$ $(S = \frac{3}{2})$ is the normalized Cr^{3+} sublattice magnetization and $\Delta E_{g2}(0)$ is the extrapolated-to-zero temperature doublet splitting in the Γ_2 phase due to the Cr-Nd coupling. A fit to the data of Fig. 5 gives

$$\Delta E_{g2}(0)/k_B = 23.6 \pm 0.4\ ^\circ\mathrm{K}\ , \tag{2}$$

where k_B is the Boltzmann constant. Thus, in the Γ_2 phase, the splitting is essentially proportional to the sublattice magnetization of the Cr^{3+} spins. No evidence for an additional polarization due to a Nd-Nd interaction is found in this temperature range. Below T_R, on the other hand, the ground-state splitting increases with decreasing temperature. Since the Cr^{3+} moments are saturated for $T < T_R$ and are in a pure G_y mode, this indicates that there exists an Nd-Nd interaction which results in a further polarization of the rare-earth spins. In the molecular-field approximation, this additional polarization will be simply proportional to the Nd sublattice magnetization. We then have

$$\Delta E_g(T) = \Delta E_{g1}^{\mathrm{Cr}}(0)(\langle S\rangle/S) + \Delta E_{g1}^{\mathrm{Nd}}(0)\tanh[\Delta E_g(T)/2k_BT], \quad T < T_R\ , \tag{3}$$

where $E_{g1}^{\mathrm{Cr}}(0)$ and $E_{g1}^{\mathrm{Nd}}(0)$ are the splittings caused by the Nd-Cr and Nd-Nd interactions, respectively, at $T = 0\ ^\circ\mathrm{K}$ in the Γ_1 phase. For $T < T_R$, the factor $\langle S\rangle/S$ is essentially unity and a least-squares fit to the data of Fig. 5 yields

$$\Delta E_{g1}^{\mathrm{Cr}}/k_B = 25.2 \pm 0.3\ ^\circ\mathrm{K}\ , \qquad \Delta E_{g1}^{\mathrm{Nd}}/k_B = 2.0 \pm 0.5\ ^\circ\mathrm{K}\ . \tag{4}$$

The magnitude of the Cr-Nd interaction in $NdCrO_3$ given by Eq. (2) may be compared with the corresponding Γ_2 phase doublet splitting of $1.6\ ^\circ\mathrm{K}$ induced by the Fe-Nd coupling in $NdFeO_3$.[21] A further comparison may be made between the $25.2\ ^\circ\mathrm{K}$ value given in Eqs. (4) and the $0\ ^\circ\mathrm{K}$ Γ_1 phase doublet splitting of $9.6\ ^\circ\mathrm{K}$ induced by the Cr-Er interaction in $ErCrO_3$.[12]

The two features discussed above, that is, the temperature dependence of the spontaneous magnetization and the ground doublet splitting, will be shown to be consistent with the following analysis, based on single ion effective field models for the Γ_1 and Γ_2 phases. We shall assume that the Γ_2 phase canting angle, i.e., the angle α between the Cr^{3+} sublattice moment and the c axis, is temperature independent. This assumption has been shown to hold for the rare-earth orthoferrites[21,23] and orthochromites.[9–13] Since, however, it implies that the transition-metal spin system is unaffected by the transition-metal rare-earth interaction, which is particularly strong in $NdCrO_3$, it is not immediately obvious that α is temperature independent in this case. The fact that the Γ_2-phase ground-doublet splitting is proportional to the Cr^{3+} sublattice moment (i.e., is apparently unaffected by the Cr-Nd coupling) provides the justification for using a constant canting angle model here.

A. Spontaneous magnetization in the Γ_2 phase

The temperature dependence of the ground doublet splitting, as given in Fig. 5, shows that (i) the Nd-Nd coupling is negligible above T_R and that (ii) $\Delta E_g(T)$ is well described by Eq. (1). Thus, to calculate the free energy F of the Nd spin system, we need only consider the effective field at a given Nd^{3+} site due to the ordered Cr spins and the applied field. In our model, we shall take into account the contributions to F arising from the occupation of the two lowest-lying crystal-field doublets of $^4I_{9/2}$, with the assumption that contributions from higher-lying states are negligible for $T < T_N$. The total free energy per mole of the Nd system is then given by

$$F = -\tfrac{1}{2}Nk_BT\{\ln\{2[\cosh(\Delta E_g^+/2k_BT) + e^{-\delta/k_BT}\cosh(\Delta E_e^+/2k_BT)]\} + \ln\{2[\cosh(\Delta E_g^-/2k_BT) + e^{-\delta/k_BT}\cosh(\Delta E_e^-/2k_BT)]\}\}. \quad (5)$$

Here N is Avogadro's number, δ is the crystal-field splitting between doublets I and II, and ΔE_g and ΔE_e refer to the Zeeman splittings of doublets I and II, respectively. In the Γ_2 phase the Zeeman splittings are related to the magnetic fields by

$$\Delta E_i^{\pm}(\vec{H}, T) = \mu_B[g_{xi}^2(H_i^{Cr}\cos\theta_i + H_a\cos\phi_i \pm H_b\sin\phi_i)^2 + g_{yi}^2(H_i^{Cr}\sin\theta_i + H_a\sin\phi_i \pm H_b\cos\phi_i)^2 + g_{zi}^2H_c^2]^{1/2}, \quad i = g, e, \quad (6)$$

where μ_B is the Bohr magneton; $H_i^{Cr}(T)$ is the magnitude of the effective field due to the Cr spin system; and H_a, H_b, and H_c are the components of the applied field $\vec{H}$ along the crystallographic axes. The $g_{\alpha i}$ ($\alpha = x, y, z$; $i = g, e$) are the principal g factors and angles θ_i and ϕ_i are defined in Fig. 6. In Fig. 6, we see that there are two inequivalent Nd^{3+} sites in a given unit cell and that the principal axes of the g tensor for a given doublet are symmetrically disposed at an angle ϕ_i with respect to the a axis. Further, for a given doublet the magnitude of H_i^{Cr} is identical at all Nd^{3+} sites and its angle with a at inequivalent sites is disposed symmetrically. It follows that the two types of sites are inequivalent with respect to a field applied along b and this is reflected by the $\pm$ signs in Eq. (6). Note that neither H_i^{Cr}, θ_i, or ϕ_i need necessarily have the same value for both doublets.

Using Eqs. (5) and (6), the contribution of the Nd spin system to the spontaneous weak ferromagnetic moment is found from

$$M_a^{Nd}(T) = -\left(\frac{\partial F}{\partial H_a}\right)_{H=0}. \quad (7)$$

Using the constant canting angle assumption discussed earlier, the total spontaneous magnetization is given by

$$M_a(T) = M_a^{Nd}(T) + M_a^{Cr}(T) = M_a^{Nd}(T) + 3\mu_B N(\langle S\rangle/S)\sin\alpha. \quad (8)$$

In Eq. (8), the Cr^{3+} g factor has been taken equal to its spin only value of 2. The temperature dependence of $\langle S\rangle/S$ can be found either from the molecular-field approximation or, alternatively, from the experimentally measured spontaneous magnetization of an orthochromite such as[24] $LuCrO_3$ with a diamagnetic rare earth. In the latter case, which was chosen here, the measured $LuCrO_3$ magnetization was normalized to unity at $T = 0\,^\circ K$, and a reduced temperature scale T/T_N was used for both compounds.

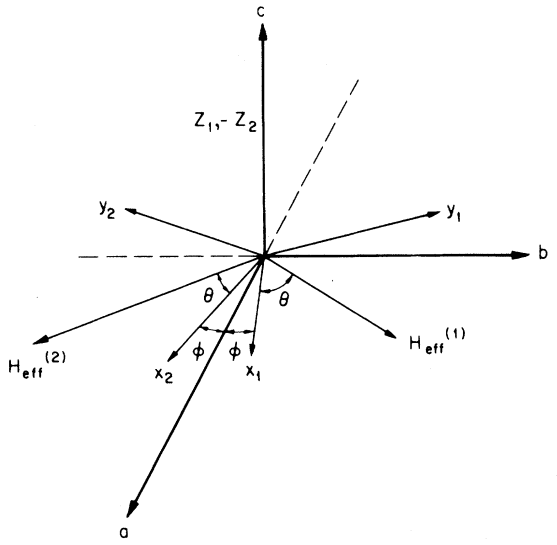

FIG. 6. Local principal magnetic axes (x_i, y_i, z_i) for two inequivalent Nd^{3+} sites in $NdCrO_3$ and effective fields $H_{eff}^{(1)}$, $H_{eff}^{(2)}$ in the $\Gamma_2(F_x)$ phase.

Due to the large number of adjustable parameters, it was not practical to use Eqs. (7) and (8) directly to obtain a fit to the measured spontaneous magnetization curve of Fig. 1. Instead, we chose first to utilize the results of the optical studies given in Figs. 4 and 5 to simplify our expression for M_a. From the data of Fig. 5 and Eq. (2), we see that $\Delta E_g(T)/k_B = \Delta E_g^+(H = 0, T)/k_B$ is less than $24\,^\circ K$ for $T > T_R$. Further, an analysis of the IIa and IIb transitions shown in Fig. 4 yields

$$\Delta E_e(T = 77\,^\circ K)/k_B = \Delta E_{e2}(T = 77\,^\circ K)/k_B = 27 \pm 3\,^\circ K. \quad (9)$$

Since $\Delta E_e(T)$ will also have a $\langle S\rangle/S$ temperature dependence and $T_N = 214\,^\circ K$, it follows from Eq. (9) that $\Delta E_e(T)/k_B$ is less than $27\,^\circ K$ for all $T > T_R$. Setting $X = \Delta E_g(T)/2k_BT$ and $\Delta E_e(T)/2k_BT$, we conclude that X is less than 0.4 for $T \geq T_R$ for either case. We can therefore approximate $\tanh X$ by X. The resulting expression for $M_a(T)$ is

$$M_a(T) = \frac{N\mu_B}{4k_BT}\frac{\Delta E_g(T)\bar{g}_g + \Delta E_e(T)\bar{g}_e\exp(-\delta/k_BT)}{1 + \exp(-\delta/k_BT)} + 3\mu_B N\left(\frac{\langle S\rangle}{S}\right)\sin\alpha, \quad (10)$$

where

$$\bar{g}_i = (g_{xi}^2\cos\theta_i\cos\phi_i - g_{yi}^2\sin\theta_i\sin\phi_i) \times[(g_{xi}^2\cos^2\theta_i + g_{yi}^2\sin^2\theta_i)^{1/2}]^{-1}, \quad i = g, e. \quad (11)$$

The effective fields H_i^{Cr}, which arise from the bilinear Cr-Nd coupling, are also proportional to $\langle S\rangle/S$ for a constant canting angle model. From

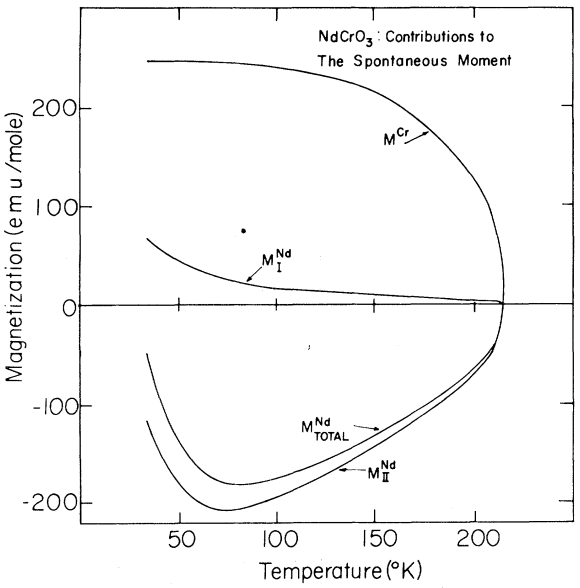

FIG. 7. Temperature dependence of the contributions to the spontaneous magnetization of $NdCrO_3$ between $T_R = 34\,^\circ K$ and $T_N = 214\,^\circ K$. M^{Cr}, M_I^{Nd}, and M_{II}^{Nd} refer to the contributions from the Cr spin system and doublets I and II of the Nd spin system, respectively. $M_{total}^{Nd} = M_I^{Nd} + M_{II}^{Nd}$.

Eq. (6), with $\vec{H} = 0$, it follows immediately that

$$\Delta E_i(T) = \Delta E_{i2}(0)(\langle S\rangle/S) , \tag{12}$$

where $\Delta E_{i2}(0)$ are the $0\,^\circ K$ zero-applied-field doublet energy splittings in the Γ_2 phase.

The final result for $M_a(T)$, as given by Eqs. (10) and (12), was fitted to the experimental data of Fig. 1 using a least squares technique with $\Delta E_{g2}(0)\bar{g}_g$, $\Delta E_{e2}(0)\bar{g}_e$, δ, and α as adjustable parameters. In fact, we could have reduced the number of parameters by one by taking $\delta/k_B = 114 \pm 7\,^\circ K$, as determined directly from the optical data of Fig. 4. However, as this value is based upon a very small amount of experimental data, we preferred to treat δ as a free parameter in our analysis. A best fit was obtained with

$$\begin{aligned} &\Delta E_{g2}(0)\,\bar{g}_g/k_B = 1.8 \pm 0.3\,^\circ K , \\ &\Delta E_{e2}(0)\bar{g}_e/k_B = -51.9 \pm 0.5\,^\circ K , \\ &\delta/k_B = 97 \pm 15\,^\circ K , \\ &\alpha = 15 \pm 1 \text{ mrad}. \end{aligned} \tag{13}$$

The quoted errors are statistical and indicate two standard deviations. The negative sign of $\Delta E_{e2}(0)\bar{g}_e$ implies that the contribution to the net magnetization from doublet II is opposite in direction to that from doublet I. Note also that the value of δ given in Eq. (13) is the same as that obtained from the optical data to within the quoted error limits.

Using Eqs. (10), (12), and (13), the total magnetization was calculated for $T_N \geq T \geq T_R$. The resulting curve is shown in Fig. 1. The fit to the experimental data is excellent. We also show, in Fig. 7, the respective contributions to the total magnetization from the Cr spin system and doublets I and II of the Nd spin system for $T > T > T_R$. The necessity of considering the doublet-II contribution in order to account for the minimum at $T \simeq 80\,^\circ K$ is clear.

B. Principal susceptibilities in the Γ_1 and Γ_2 phases

The two doublet model for the spontaneous magnetization must, of course, also allow us to calculate the temperature dependence of the principal susceptibilities. We consider first the temperature region above T_R where $NdCrO_3$ is in the Γ_2 phase. The contribution of the Nd spin system to the principal susceptibilities is given by

$$\chi_j^{Nd} = -\left(\frac{\partial^2 F}{\partial H_j^2}\right)_{H=0} , \quad j = a, b, c . \tag{14}$$

Making the same high-temperature expansion as in Sec. III A and keeping only the leading terms yields

$$\chi_j^{Nd} = \frac{N\mu_B^2}{4k_BT}\,\frac{g_{jg}^2 + e^{-\delta/k_BT} g_{je}^2}{1 + e^{-\delta/k_BT}} , \tag{15}$$

where

$$\begin{aligned} g_{ai} &= g_{xi}^2 \cos^2\phi_i + g_{yi}^2 \sin^2\phi_i , \\ g_{bi} &= g_{xi}^2 \sin^2\phi_i + g_{yi}^2 \cos^2\phi_i , \\ g_{ci} &= g_{zi} , \quad i = g, e . \end{aligned} \tag{16}$$

For temperatures below T_R, the Nd spin system has a c_z structure and the expression for this system's free-energy contribution must be modified accordingly. While the high-temperature expansion used for the Γ_2 phase is no longer valid, we can simplify the Γ_1 free-energy expression by taking only the contribution from the lowest-lying Kramers doublet. This is reasonable since for $T \leq T_R$ the quantity $\exp(-\delta/k_BT) \leq 0.06$. In addition, since $\Delta E_g(T)$, $T < T_R$ in Fig. 5 shows evidence of an additional polarization of the Nd spin system due to Nd-Nd coupling, the contribution from this coupling term should also be considered. This was done earlier in Eq. (3) in our analysis of the $\Delta E_g(T)$, $T < T_R$ data. However, this analysis showed that the Nd-Nd contribution to the over-all splitting is only 8% of that due to the Cr-Nd coupling. We shall therefore simplify our analysis of the susceptibility data further by neglecting this small contribution. The resulting calculation is then straightforward[10,21] and yields

$$\chi_j^{\mathrm{Nd}} = \frac{N\mu_B^2 g_{jg}^2}{2\Delta E_{g1}(0)} \tanh\left(\frac{\Delta E_{g1}(0)}{2k_B T}\right), \quad j = a, b,$$
$$\chi_c^{\mathrm{Nd}} = \frac{N\mu_B^2 g_{cg}^2}{4k_B T} \operatorname{sech}^2\left(\frac{\Delta E_{g1}(0)}{2k_B T}\right). \tag{17}$$

In Eq. (17), we have taken $\Delta E_{g1}(T) = \Delta E_{g1}(0)$ for $T < T_R$.

The measured $NdCrO_3$ susceptibilities include, of course, contributions from the Cr^{3+} as well as the Nd^{3+} ions. The Cr^{3+} contribution to each of the measured susceptibilities is relatively small and was simply taken to have a constant temperature-independent value of

$$\chi_i^{\mathrm{Cr}} = 4\times 10^{-3} \text{ emu/mole}, \quad i = a, b, c. \tag{18}$$

This is essentially the perpendicular susceptibility of $LuCrO_3$,[24] after a suitable normalization of the temperature scale to a T_N of 214 °K.

The fit to the measured susceptibilities was carried out in two stages. First the Γ_1 phase region was considered and the expression $\chi_j = \chi_j^{\mathrm{Cr}} + \chi_j^{\mathrm{Nd}}$ was fitted to the data using Eqs. (17) and (18) with g_{jg}, $j = a, b, c$ as the adjustable parameters. The splitting $\Delta E_{g1}(0)$ was taken from Eqs. (4). A computerized least-squares technique was employed for χ_b and χ_c while χ_a was fitted asymptotically to the low-temperature data. The latter procedure was necessary for χ_a as the spin structure tends to return to the Γ_2 phase in the temperature region immediately below T_R when a field is applied along the a axis. A best fit was obtained with

$$g_{ag} = 2.3 \pm 0.3, \quad g_{bg} = 2.7 \pm 0.1, \quad g_{cg} = 3.3 \pm 0.6. \tag{19}$$

Next, the Γ_2 phase-temperature-region data were analyzed using Eqs. (15) and (18) with g_{je}, $j = a, b, c$ as the parameters. Values for δ and g_{jg} were taken from Eqs. (13) and (19), respectively. A best fit was obtained with

$$g_{ae} = 5.4 \pm 0.5, \quad g_{be} = 5.2 \pm 0.5, \quad g_{ce} = 2.6 \pm 2.6. \tag{20}$$

Using Eqs. (15) and (17)–(20), the principal susceptibilities were calculated for $4.2\,^{\circ}\mathrm{K} < T < T_N$. The results obtained are shown in Fig. 2. The fit is, generally speaking, excellent except for χ_a immediately below T_R. The reason for this was noted previously.

IV. DISCUSSION

In our analysis of the experimental optical and magnetic data for $NdCrO_3$ in its Γ_1 and Γ_2 phases, we showed that a satisfactory explanation of the observed behavior could be found within the framework of a single-ion effective-field model. The additional factor essential to our analysis was the need to consider, for the case of $NdCrO_3$, the contribution from two rather than only one Kramers doublet of the Nd^{3+} ground term. This had not been found to be necessary previously when studying other odd electron systems, such as Nd^{3+} in $NdFeO_3$,[21] and Er^{3+} in $ErCrO_3$.[12] The distinguishing factor between $NdCrO_3$ and these other compounds is the extremely strong rare-earth transition-metal coupling present in the former. For the Γ_1 phase, we can calculate the magnitude of the effective field $H_{g1}^{\mathrm{Cr}}(0)$ acting on the ground doublet at 0 °K from

$$k_B \Delta E_{g1}^{\mathrm{Cr}}(0) = g_{cg}\mu_B H_{g1}^{\mathrm{Cr}}(0). \tag{21}$$

Using Eqs. (4), (19), and (21) gives

$$H_{g1}^{\mathrm{Cr}}(0) = 115 \pm 25 \text{ kOe}. \tag{22}$$

Comparable values for $NdFeO_3$ in its Γ_2 and Γ_4 phases are 8.6 and 3.1 kOe, respectively.[21] For the orthochromites, the largest rare-earth transition-metal coupling fields reported previously are 12.6 and 11.7 kOe for $ErCrO_3$ in its Γ_1 and Γ_4 phases.[12] Thus the coupling field between the Cr spins and the lowest-lying doublet of Nd^{3+} in $NdCrO_3$ is an order of magnitude greater than corresponding fields in $NdFeO_3$ or $ErCrO_3$. It is reasonable to assume that the coupling field is the same for all states belonging to the same term[25] and also that the Γ_2 phase field $H_{g2}^{\mathrm{Cr}}(0) = H_{e2}^{\mathrm{Cr}}(0)$ is of the same order of magnitude as $H_{g1}^{\mathrm{Cr}}(0)$. The latter is substantiated by the observed Zeeman splittings ΔE_{g2}, ΔE_{e2} given in Eqs. (2) and (9) and also by our observation that applied fields of up to 20 kOe had no observable effect on the absorption spectra. We conclude that it is the combination of the strong Zeeman splitting ΔE_e and the relatively large ab plane g factors of doublet II in comparison with doublet I that accounts for the significant contribution of doublet II to the spontaneous magnetization of $NdCrO_3$. The opposite algebraic signs of the doublet contributions to the spontaneous magnetization, as noted in (13) and Figs. 1 and 7, result in the observed temperature dependence.

In Table I, we compare our results for doublet I of Nd^{3+} in $NdCrO_3$ with the corresponding values reported[21] for $NdFeO_3$. From Table I, we again see that the main difference between the orthochromite and the orthoferrite is in the magnitude of the Nd–transition-metal coupling. For $NdCrO_3$, our combined optical and magnetization studies have shown that the crystal-field splitting between doublets I and II is approximately 100 °K. The comparable value for $NdFeO_3$ is not known. However, for Nd^{3+} in the isostructural compounds $YAlO_3$ and $NdAlO_3$, splittings of[26] 168 °K and[27] 176 °K have been reported. These somewhat larger Nd^{3+} splittings in the orthoaluminates as compared with the orthochromites (or orthoferrites) are not unexpected as similar results have been reported, for example, in the case of Er^{3+} in $ErCrO_3$,[12,28] $ErFeO_3$,[18,25] and $ErAlO_3$.[29]

TABLE I. Comparison of $NdCrO_3$ with $NdFeO_3$ [g_a, g_b, and g_c are the g factors of the lowest-lying Kramers doublet of Nd^{3+} along the a, b, and c crystallographic axes, respectively, and $\Delta E_g(0)$ is the extrapolated-to-0 °K Zeeman splitting of the same doublet in the $\Gamma_2(Cr^{3+}: G_zF_x$; $Nd^{3+}: c_yf_x)$ phase due to the coupling of the Nd moments to the transition-metal spin system].

	$NdCrO_3$ [a]	$NdFeO_3$ [b]
g_a	2.3 ± 0.3	2.4 ± 0.3
g_b	2.7 ± 0.1	3.6 ± 0.4
g_c	3.3 ± 0.6	2.5 ± 0.2
$\Delta E_g(0)/k_B$ (°K)	23.6 ± 0.1	1.6 ± 0.2

[a]This work [b]Reference 21.

From the discontinuity in the ground-doublet splitting at T_R, the difference in the anisotropy energy ΔK of the Cr^{3+} spin system in the two phases can be calculated.[30] (The contribution of doublet II at this temperature is negligible.) The spin reorientation takes place at constant (zero) external field and temperature with no apparent hysteresis, thus the magnetic analog of the Gibbs free energy is continuous at the phase transition. For the Γ_2 phase[12]

$$F(\Gamma_2) = -\tfrac{9}{4}\lambda(\mu_B N)^2 - \tfrac{9}{8}(\mu_B N)^2 D^2/\lambda - K(\Gamma_2) - Nk_BT_R \ln\{2\cosh[\Delta E_{g2}(T_R)/2k_BT_R]\}, \quad (23)$$

where we have set $\langle S\rangle = S$ at $T = T_R$ and $K(\Gamma_2)$ is the Γ_2 phase anisotropy energy. The Heisenberg and Dzialoshinsky exchange constants λ and D can be found directly from the canting angle $\alpha = 15$ mrad and Néel temperature $T_N = 214$ °K by using the relations[12,21]

$$T_N = 5N\mu_B^2\lambda/4k_B\,, \quad \alpha = D/2\lambda\,. \quad (24)$$

In Eqs. (23) and (24), we have taken $S = \frac{3}{2}$ and the g factor of the Cr^{3+} moments equal to 2. Similarly, for the Γ_1 phase[12]

$$F(\Gamma_1) = -\tfrac{9}{4}\lambda(\mu_B N)^2 - K(\Gamma_1) - Nk_BT_R \ln\{2\cosh[\Delta E_{g1}(T_R)/2k_BT_R]\} + \tfrac{1}{4}N\Delta E_{g1}^{Nd}(0)\tanh^2[\Delta E_{g1}(T_R)/2k_BT_R]. \quad (25)$$

Setting $F(\Gamma_2) = F(\Gamma_1)$ and taking $T_R = 35.1$ °K, $\Delta E_{g2}(T_R)/k_B = 23.6$ °K, $\Delta E_{g1}(T_R)/k_B = 25.9$ °K, $\Delta E_{g1}^{Nd}(0)/k_B = 2.0$ °K, $\lambda = 226$ Oe mole/emu, and $D = 6.9$ Oe mole/emu, we obtain

$$\frac{\Delta K}{Nk_B} = \frac{K(\Gamma_1) - K(\Gamma_2)}{Nk_B} = 0.25 \pm 0.05\ ^\circ\text{K/spin}. \quad (26)$$

This result may be compared with that found for the spontaneous $\Gamma_4 \rightleftharpoons \Gamma_1$ phase transition in $ErCrO_3$ where values of 0.57 ± 0.15,[12] 0.45 ± 0.08,[28] and[3] 0.45 °K/spin have been reported.

We can also evaluate $T_R\Delta\sigma$, the latent heat associated with the spin reorientation. Since the Cr spin system is essentially completely ordered at $T = T_R$, we can neglect its contribution to the entropy change. We then have

$$T\Delta\sigma = \Delta U - \Delta F = [U(\Gamma_1) - U(\Gamma_2)] - [F(\Gamma_1) - F(\Gamma_2)]\,, \quad (27)$$

where U is the internal energy of the system. Since $F(\Gamma_1) = F(\Gamma_2)$ at $T = T_R$, we obtain[12]

$$T\Delta\sigma = -\tfrac{1}{2}N\Delta E_{g1}(T_R)\tanh[\Delta E_{g1}(T_R)/2k_BT_R] - \tfrac{1}{4}N\Delta E_{g1}^{Nd}(0)\tanh^2[\Delta E_{g1}(T_R)/2k_BT_R] + \tfrac{1}{2}N\Delta E_{g2}(T_R)\tanh[\Delta E_{g2}(T_R)/2k_BT_R] - K(\Gamma_1) + K(\Gamma_2) - \tfrac{9}{8}(\mu_B N)^2 D^2/\lambda\,, \quad (28)$$

$$T\Delta\sigma/Nk_B = 0.37 \pm 0.05\ ^\circ\text{K/spin}\,. \quad (29)$$

This last result may be compared with the values of 0.25 ± 0.05,[12] 0.15 ± 0.05,[28] and[31] 0.2 reported for the $\Gamma_4 \rightleftharpoons \Gamma_1$ phase transition in $ErCrO_3$.

Finally, from the results of the analysis of the magnetic properties of $NdCrO_3$, the magnetic contribution to the low-temperature specific heat of this compound can be calculated. Taking the Nd-Nd interaction term into account, the Nd ground-doublet contribution to the specific heat is given by[28]

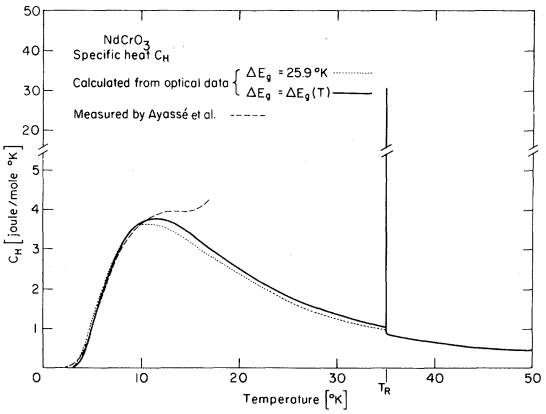

FIG. 8. Low-temperature specific heat of $NdCrO_3$. The dashed line denotes the experimental results of Ayasse (see Refs. 5 and 6) for the total specific heat. The dotted line is the calculated contribution of the Nd spin system to the specific heat, assuming that the ground-doublet splitting of the Nd^{3+} ion is temperature independent. The solid line is the contribution of the Nd spin system to the specific heat as calculated from the optical results for the temperature dependence of the ground-doublet splitting. The peak at T_R is calculated from the latent heat of the $\Gamma_2(F_x) \rightleftharpoons \Gamma_1(0)$ phase transition, assuming that the transition width is 0.1 °K at half the maximum. (Note the change in scale for C_H.)

$$C_H^{\mathrm{Nd}} = -N\Delta E_g(T)\left[1-\tanh^2\left(\frac{\Delta E_g(T)}{2k_BT}\right)\right]$$

$$\times\left[\frac{\Delta E_g(T)}{2k_BT^2}-\left(\frac{\partial\Delta E_g(T)}{\partial T}\right)\Big/\,2k_BT\right], \qquad (30)$$

where $\Delta E_g(T)$ is to be set equal to $\Delta E_{g1}(T)$ or $\Delta E_{g2}(T)$ according to whether T is less than or greater than T_R. We have used Eq. (30) to calculate C_N^{Nd} for $T<50\,^\circ$K, taking $\Delta E_g(T)$ directly from the optical data given in Fig. 5. For comparison, we have also calculated C_N^{Nd} assuming a temperature independent doublet splitting of 25.9 °K. The results are shown in Fig. 8 where the experimental results of Ayasse *et al.*[5,6] for $T<17\,^\circ$K are also given. The latter of course also includes contributions from the Cr spin system and the lattice. To our knowledge, no specific-heat studies have been carried out in the vicinity of the $NdCrO_3$ phase transition at T_R.

In conclusion, by means of combined absorption spectroscopy, and bulk magnetization measurements, the magnetic properties of $NdCrO_3$ have been studied as a function of temperature. We have found that these properties can be understood in terms of a single-ion model which treats the interactions between the electrons occupying the two lowest-lying Kramers doublets of the Nd^{3+} ion and the Cr^{3+} and Nd^{3+} spin systems by means of effective fields. A spontaneous Morin-type spin-reorientation phase transition occurs at 35.1 °K from a weak-ferromagnetic high-temperature state to an antiferromagnetic low-temperature one. The transition appears to be of first order. The ferrimagneticlike temperature dependence of the magnetization above the spin reorientation is due to the extremely strong coupling between the Nd and Cr spin systems.

ACKNOWLEDGMENTS

We are grateful to Professor S. Shtrikman and Professor D. Teves for many helpful discussions and suggestions during the course of this work, and to Y. Chopen and D. Leibowitz for technical assistance.

*Present address: High Power Laser Laboratory, Soreq Nuclear Research Center, Yavne, Isreal.
†Present address: University of Surrey, Guildford, Surrey GU2 5XH, England.
‡Present address: Dept. of Physics, University of Manitoba, Winnipeg, Manitoba, Canada.

[1]S. Geller and E. A. Wood, Acta Crystallogr. 9, 563 (1956); S. Geller, J. Chem. Phys. 24, 1236 (1956); E. F. Bertaut and F. Forrat, J. Phys. Radium 17, 129 (1956).
[2]E. F. Bertaut, J. Mareschal, G. de Vries, R. Aleonard, R. Pauthenet, J. P. Rebouillat, and J. Sivardiere, IEEE Trans. Magn. 2, 453 (1966).
[3]E. F. Bertaut and J. Mareschal, Solid State Commun. 5, 93 (1967).
[4]P. Patand and J. Sivardiere, J. Phys. (Paris) 31, 803 (1970).
[5]J. B. Ayasse, A. Berton, and J. Sivardiere, C. R. Acad. Sci. (Paris) B 271, 1220 (1970).
[6]J. B. Ayasse, Ph.D. thesis (University of Grenoble, 1970) (unpublished).
[7]E. C. Koehler, E. O. Wollan, and M. K. Wilkinson, Phys. Rev. 118, 58 (1960); E. F. Bertaut, in *Magnetism*, edited by G. T. Rado and H. Suhl (Academic, New York, 1963), Vol. III, p. 149.
[8]The double subscript on G_{xy} denotes that the antiferromagnetic axis lies in the xy plane; we use upper case letters (i.e., G) to designate Cr spin configurations and lower case (i.e., c) to denote Nd spin configurations.
[9]S. Shtrikman, B. M. Wanklyn, and I. Yaeger, Int. J. Magn. 1, 327 (1971).
[10]R. M. Hornreich, B. M. Wanklyn, and I. Yaeger, Int. J. Magn. 2, 77 (1972).
[11]R. M. Hornreich, B. M. Wanklyn, and I. Yaeger, Int. J. Magn. 4, 313 (1973).
[12]A. Hasson, R. M. Hornreich, Y. Komet, B. M. Wanklyn, and I. Yaeger, Phys. Rev. B (to be published).
[13]J. D. Gordon, R. M. Hornreich, S. Shtrikman, and B. M. Wanklyn, Phys. Rev. B (to be published).
[14]K. P. Belov, M. A. Belyanchikova, A. M. Kadomtseva, I. B. Krynetskii, T. M. Ledneva, T. L. Ovchimmikova, and V. A. Timofeeva, Fiz. Tverd. Tela 14, 248 (1972) [Sov. Phys.-Solid State 14, 199 (1972)].
[15]R. M. Hornreich, Y. Komet and B. M. Wanklyn, Solid State Commun. 11, 969 (1972).
[16]M. Eibschütz, Acta Crystallogr. 19, 337 (1965); P. Coppens and M. Eibschütz, *ibid.* 19, 524 (1965).
[17]G. H. Dieke and L. Heroux, Phys. Rev. 103, 1227 (1955).
[18]R. Faulhaber, S. Hüfner, E. Orlich, and H. Schubert, Z. Phyz. 204, 101 (1967).
[19]A. P. Malozemoff, Technical Report, Stanford Electronics Laboratories, Stanford, Calif., May 1970 (unpublished); J. Phys. Chem. Solids 32, 1669 (1971).
[20]R. L. White, J. Appl. Phys. 40, 1061 (1969), and references cited therein.
[21]R. M. Hornreich and I. Yaeger, Int. J. Magn. 4, 71 (1973).
[22]L. R. Maxwell and S. J. Pickart, Phys. Rev. 92, 1120 (1953).
[23]M. Eibschütz, S. Shtrikman, and D. Treves, Phys. Rev. 156, 562 (1967).
[24]I. Yaeger, Ph. D. thesis (Weizmann Institute of Science, 1973) (unpublished); R. M. Hornreich, S. Shtrikman, B. M. Wanklyn, and I. Yaeger (unpublished).
[25]D. L. Wood, L. M. Holmes, and J. P. Remeika, Phys. Rev. 185, 689 (1969).
[26]M. J. Weber and T. E. Varitimose, J. Appl. Phys. 42, 4996 (1971).
[27]E. Finkman, E. Cohen, and L. G. Van Uitert, Phys. Rev. B 7, 2899 (1973).

[28]R. Courths, S. Hüfner, J. Pelzl, and L. G. Van Uitert, Solid State Commun. 8, 1163 (1970); Z. Phyz. 249, 445 (1972).
[29]V. L. Doulan and A. A. Santiago, J. Chem. Phys. 57, 4717 (1973).
[30]This is a revised version of an earlier calculation given in Ref. 15.
[31]M. Eibschütz, L. Holmes, J. P. Maita, and L. G. Van Uitert, Solid State Commun. 8, 1815 (1970).